Conjugate heat transfer simulation of sulfuric acid condensation in a large two-stroke marine engine - the effect of thermal initial condition

Nemati, Arash; Jensen, Michael Vincent; Pang, Kar Mun; Walther, Jens Honoré

Published in:
Applied Thermal Engineering

Link to article, DOI:
10.1016/j.applthermaleng.2021.117075

Publication date:
2021

Document Version
Peer reviewed version

Journal Pre-proofs

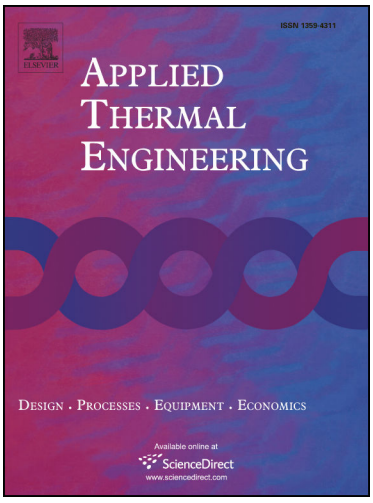

Conjugate heat transfer simulation of sulfuric acid condensation in a large two-stroke marine engine - the effect of thermal initial condition

Arash Nemati, Michael Vincent Jensen, Kar Mun Pang, Jens Honoré Walther

PII: S1359-4311(21)00518-4
DOI: https://doi.org/10.1016/j.applthermaleng.2021.117075
Reference: ATE 117075

To appear in: *Applied Thermal Engineering*

Received Date: 29 August 2020
Accepted Date: 6 May 2021

Please cite this article as: A. Nemati, M.V. Jensen, K.M. Pang, J.H. Walther, Conjugate heat transfer simulation of sulfuric acid condensation in a large two-stroke marine engine - the effect of thermal initial condition, *Applied Thermal Engineering* (2021), doi: https://doi.org/10.1016/j.applthermaleng.2021.117075

Conjugate heat transfer simulation of sulfuric acid condensation in a large two-stroke marine engine - the effect of thermal initial condition

Arash Nemati[a,*], Michael Vincent Jensen[a], Kar Mun Pang[a], Jens Honoré Walther[a,b]

[a] *Department of Mechanical Engineering, Technical University of Denmark, 2800 Kgs. Lyngby, Denmark*
[b] *Computational Science and Engineering Laboratory, ETH Zürich, CH-8092 Zürich, Switzerland*

Abstract

In the present study, conjugate heat transfer (CHT) calculations are applied in a computational fluid dynamics (CFD) simulation to simultaneously solve the in-cylinder gas phase dynamics and the temperature field within the liner of the engine. The effects of different initial temperatures with linear profiles across the liner are investigated on the wall heat transfer as well as on the sulfuric acid formation and condensation. The temporal and spatial behavior of sulfuric acid condensation on the liner suggests the importance of CHT calculations under large two-stroke marine engine relevant conditions. Comparing the mean value of the heat transfer through the inner and outer sides of the liner, an initial temperature difference of 15 K with a linear profile is an appropriate initial condition to initiate the temperature within the liner.

*I am corresponding author
Email addresses: arnem@mek.dtu.dk (Arash Nemati), mvje@mek.dtu.dk (Michael Vincent Jensen), jhw@mek.dtu.dk (Jens Honoré Walther), (Jens Honoré Walther)
URL: author-one-homepage.com (Arash Nemati)

Moreover, the effect of the amount of water vapor in the air on the sulfuric acid formation and condensation is studied. The current results show that the sulfuric acid vapor formation is more sensitive to the variation of the water vapor amount than the sulfuric acid condensation.

Keywords: Marine engine, Two stroke, Sulfuric acid, CHT, CFD

1. Introduction

The shipping industry utilizes two-stroke diesel engines as the main source of propulsion. These engines burn Heavy Fuel Oil (HFO) which contains sulfur leading to the formation of sulfur oxides (SO_x). In order to decrease the hydrodynamic drag on the ship hull and improve fuel savings, ships use a slow steaming operation strategy. An unwanted side effect of slow steaming is the formation and condensation of sulfuric acid (H_2SO_4) and water (H_2O) on the liner in the regions where the local temperature is low. This can result in cold corrosion and high liner wear rates [1]. To diminish this negative effect, lube oil containing limestone additives is utilized to neutralize the acid and decrease the corrosion of the liner. However, this method increases the operational costs. Therefore, having a better understanding of the sulfuric acid formation and condensation is essential to minimize the expenses of lubrication.

One of the main challenges is to accurately predict the SO_x formation inside the combustion chamber. A detailed hydrogen/sulfur/oxygen (H/S/O) reaction mechanism developed by Hindiyarti et al. [2] was used together with a multi-zone model for the investigation of SO_x formation under large two-stroke marine engine conditions by Cordtz et al. [3]. However, one of the

main limitations of multi-zone models is the absence of detailed information about the distribution of temperature and combustion products. Moreover, calibration of a mixing constant in the multi-zone models is required for different engine speeds [3].

On the other hand, 3D-CFD models have the capability to give a comprehensive insight into the species and temperature distribution and mixing process inside the cylinder [4]. Pang et al. [1] and Karvounis et al. [5] conducted comprehensive studies on sulfuric acid formation using a 3D-CFD method. They concluded that the in-cylinder gas is cooled rapidly when it comes in contact with the cylinder wall and sulfuric acid vapor is produced in the region where the local gas temperature is less than 600 K. Hence, the prediction of the local gas temperature near the cylinder wall as well as the wall temperature is important for an accurate estimation of the H_2SO_4 formation and condensation. Pang et al. [1] and Karvounis et al. [5] considered however a constant wall temperature in their CFD simulations due to the lack of experimental data for the wall temperature. They studied the acid formation sensitivity to the wall temperature using uniform temperature distributions on the liner surface of 323 K and 523 K, respectively. The wall temperature was found to have a major effect on the sulfuric acid formation and condensation. However, it is unrealistic to consider a uniform temperature on the liner as the temperature, in reality, varies along the liner.

To obtain a realistic wall temperature, conjugate heat transfer (CHT) calculations are essential in order to solve the energy equation in the solid phase simultaneously with the governing equations for the in-cylinder gas phase. This enables an evaluation of the heat exchange between the in-cylinder gas

and the cylinder wall to ensure an accurate calculation of the wall temperature. Jensen et al. [6] studied the effect of CHT calculations on the sulfuric acid formation. They considered a uniform temperature as well as a non-uniform temperature on the outer surface of the solid liner region. They concluded that including CHT calculations influenced to some degree the predictions of the potential sulfuric acid condensation. However, they used a constant temperature profile in the radial direction as initial temperature distribution inside the solid liner domain which may lead to a less accurate prediction of the heat transfer inside the solid liner domain and hence a non-realistic solid-gas interface temperature. Li and Kong [7] considered CHT to predict heat conduction in the solid domain and studied the effects on combustion and emission. They initiated their solid domain with an uniform temperature. They used a coarse mesh and they repeated their simulation for 70 engine cycles. They concluded that using the CHT model does not significantly change the predictions of the global engine combustion and emissions parameters. Zhang [8] carried out a parallel simulation of engine in-cylinder processes with CHT modeling. A mesh consisting of 12080 cells for the fluid domain and 5286 cells for the solid domain was used and the simulation was repeated for 80 engine cycles. Based on the results, considering CHT calculations has a strong impact on the prediction of the in-cylinder dynamics in the fluid phase in comparison with the baseline simulation assuming a constant wall temperature. Vincekovic [9] conducted a numerical simulation with CHT calculations on the piston cooling of a two-stroke marine diesel engine. An initial temperature inside the piston obtained from experimental measurements was considered and the heat transfer obtained from the numer-

ical results was compared with experimental measurements for a full engine cycle. Berni et al. [10] carried out a combined in-cylinder/CHT simulation loop for an engine and proposed a modified thermal wall function. They compared the target heat transfer from a thermal balance and the obtained cycle-averaged heat transfer from a full-cycle simulation for different heat transfer models. It is concluded that the proposed model leads to computed heat fluxes much closer to the target value than Angelberger's and Han and Reitz's models.

Based on the aforementioned literature review, prediction of SO_x and H_2SO_4 formation during combustion needs an appropriate chemical mechanism. On the other hand, to obtain an estimation of the H_2SO_4 condensation, an appropriate liner wall temperature is necessary which can be obtained using CHT calculations. Therefore, a 3D-CFD model with CHT calculations is utilized in this study to estimate the H_2SO_4 formation and condensation on the liner under large two-stroke marine engine like conditions. To obtain a realistic liner temperature profile in radial direction inside the solid liner domain for CHT calculations, it is advised to carry out a full cycle simulation for several cycles to obtain a periodic steady state temperature distribution [7, 8] or impose initial conditions obtained from experimental measurements [9]. However, this is computationally expensive, especially when using a complex chemical mechanism in the CFD analysis of large marine engines. A significant amount of experimental data is also needed to simulate the full cycle, including the scavenging process, properly. Considering an approximation for the initial temperature distribution inside the solid liner domain could be a solution to reduce the computational expenses.

Therefore, in this study, various initial temperature differences with a linear profile across the solid liner domain are investigated to mimic the accumulated effect of previous cycles on the internal temperature of the liner. A sensitivity analysis is carried out on the associated influence of the initial temperature difference on the heat transfer and sulfuric acid formation and condensation. Moreover, the influence of the water vapor amount in the cylinder gas at the start of the simulation on the sulfuric acid formation and condensation is studied to represent the effect of ambient air conditions. Finally, the spatial distribution of the sulfuric acid vapor and the distribution of the condensed H_2SO_4 on the liner surface are presented at various times during the combustion period.

2. Numerical modeling

A 3D-CFD study is performed using the commercial CFD code STAR-CCM+ version 13.06.012-R8 to simulate the two-stroke test engine 4T50ME-X located at MAN Energy Solutions in Denmark [4], operating under full load condition. Details of the engine specifications are presented in Table 1. The turbulent flow is modeled using the Unsteady Reynolds Averaged Navier-Stokes (URANS) method with the k-ω Shear Stress Transport (SST) model [11]. For diesel spray modeling, the Rosin-Rammler model is utilized to model the initial droplet size distribution and the Kelvin Helmholtz-Rayleigh Taylor (KH-RT) model is applied to simulate the diesel fuel spray secondary breakup. In this study, the diesel fuel is chemically represented by n-heptane fuel while the liquid properties of tetradecane ($C_{14}H_{30}$) are used due to the similarity between the thermo-physical properties of $C_{14}H_{30}$ and diesel fuel

[4]. A reduced n-heptane chemical kinetic mechanism with 37 species including a sulfur chemistry subset is used for modeling the formation of SO_x and subsequently sulfuric acid vapor. Detailed explanations about the models and operating conditions can be found in the previous works [1, 4]. For the CHT simulation, a 5 mm layer of cast iron is considered to represent the cylinder liner [6]. The temperature boundary condition of the outer surface of the solid liner domain is assumed to follow a second order polynomial function based on measurements recorded at 5 mm into the liner from the gas-liner interface [12]:

$$T(z) = az^2 - bz + c \tag{1}$$

where $a = 40\,\mathrm{K/m^2}$; $b = 180\,\mathrm{K/m}$, and $c = 523\,\mathrm{K}$, T is the temperature in Kelvin (K), and z is the distance from the cylinder cover towards the scavenge ports in meters (m). An initial temperature difference across the solid liner domain is imposed to mimic the accumulated effect of previous cycles on the internal temperature of the liner. The symmetry obtained by the use of two identical injectors in the engine allows a 180° sector mesh (shown in Figure 1) to be used to represent half of the combustion chamber. The location of the injector and the direction of the nozzle holes are also illustrated in Figure 1-b with blue arrows. The mesh size inside the gas domain is $0.01\times D$ (D is the cylinder diameter) which is refined to $0.005\times D$ around the injector. To resolve the thermal wall boundary layer, 20 prism layers are used in the gas phase. A sensitivity analysis of the number of prism layers can be found in our previous study [1]. In the radial direction, 20 layers of cells are used inside the solid domain and in the axial direction, the solid domain consists

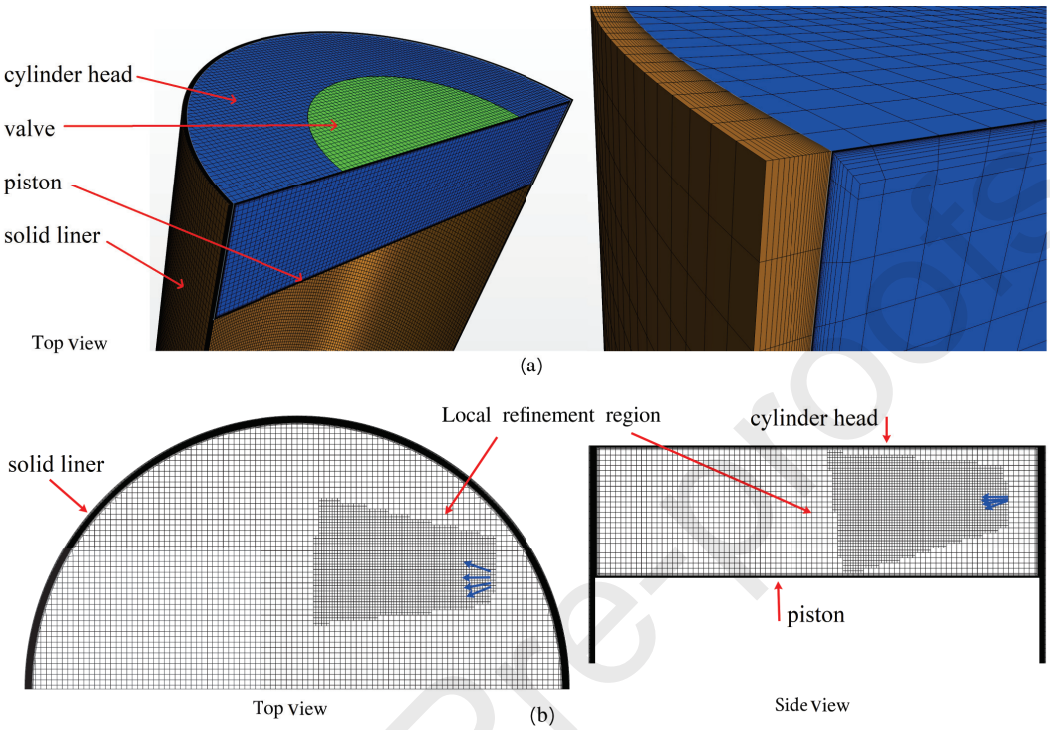

Figure 1: a) left: overview of mesh and solid surfaces, right: close-up on the cylinder mesh (in blue) and solid liner mesh (in brown). b) cross sections of the computational grid.

of 340 layers. The total number of cells in the fluid domain is 406075 at TDC and there are 1352000 cells in the solid domain.

3. Results and discussion

3.1. Validation

The numerical model is validated by comparing the in-cylinder pressure trace at 100 % load obtained from the CFD simulation with experimental measurements. It can be seen from Figure 2 that there is a good agreement between the CFD result and the experimental measurement. Validation of

Table 1: 4T50ME-X engine specifications and operating conditions used in the current simulations.

Parameter	
Bore	500 mm
Stroke	2200 mm
Connecting rod length	2885 mm
Engine load	100 %
Engine speed	123 rpm
Start of fuel injection	1.2 CAD ATDC
Injection duration	31.2 ms
Fuel temperature	400 K
Nozzle hole diameter	1.05 mm

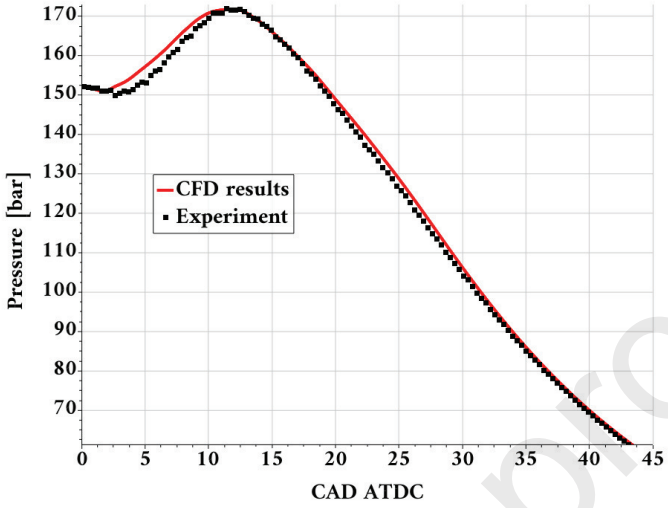

Figure 2: Comparison of the in-cylinder pressure trace obtained from the CFD simulation and experimental measurements [4].

the conversion rate of SO_2 to SO_3 is presented in our previous study [1] (not shown).

3.2. Initial temperature distribution

In this section, the effect of the initial temperature difference across the solid liner domain is investigated to obtain an appropriate estimation of the temperature distribution inside the solid liner domain. Due to the high computational cost of solving chemical reactions, only the combustion phase and a part of the expansion phase is simulated from 0 crank angle degrees (CAD) after top dead center (ATDC) to 90 CAD ATDC. Keeping the same temperature boundary condition for the outer surface of the solid liner domain, we consider three linear temperature profiles within the solid liner domain with the thickness of 5 mm corresponding to temperature differences across the liner domain of 0 K, 15 K, and 25 K which is illustrated in Figure 3. These

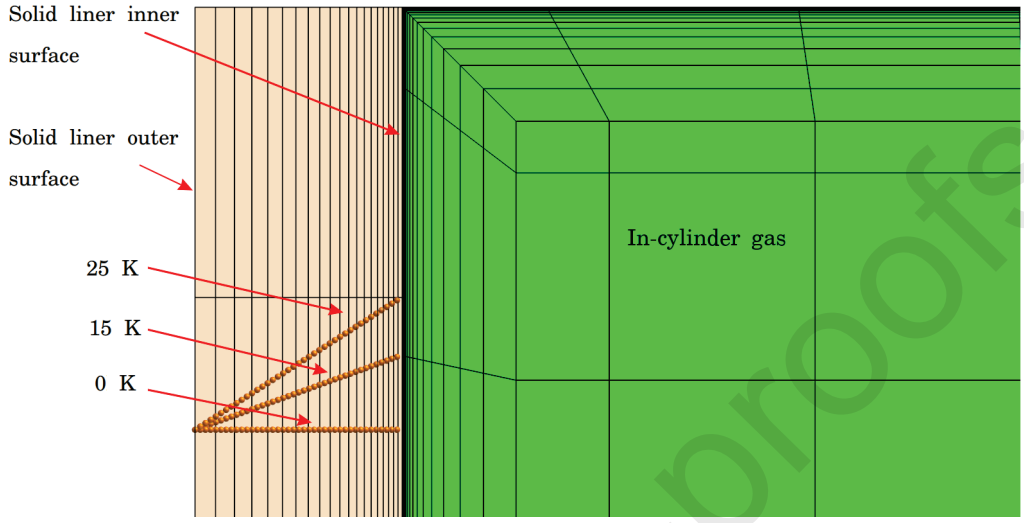

Figure 3: Initial temperature difference across the solid liner domain - 0 K, 15 K and 25 K.

temperature differences are considered to represent the influence of previous cycles on the internal liner temperature.

The total wall heat transfer from the in-cylinder gas to the liner for the three initial temperature differences is illustrated in Figure 4. As it can be seen, the maximum heat transfer occurs around 30 CAD ATDC, where the flame has the highest interaction with the liner. The mean value of the interface heat transfer from 0 to 90 CAD ATDC is 181.5 kW, 177.9 kW and 173.6 kW for the initial temperature difference of 0 K, 15 K, and 25 K, respectively. Due to the short physical time of the simulated part of the engine cycle (0.122 s for 90 CAD), the time for diffusion of heat inside the solid liner domain is limited, and the heat flow out of the outer side of the solid domain remains approximately constant for all CAD. The associated heat transfer rate is 1 kW, 177 kW, and 294 kW for the 0 K, 15 K, and 25 K cases, respectively. Considering a balance between the mean value of heat

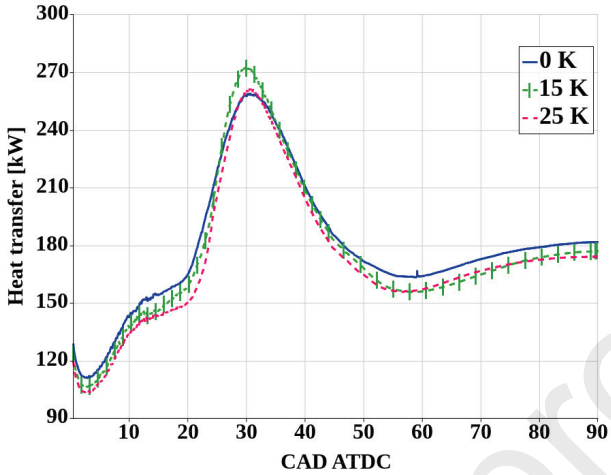

Figure 4: Heat transfer at the gas-liner interface.

transfer to and from the solid liner domain, the mean value of the heat transfer at the solid-gas interface and at the outer surface of the solid liner domain should be balanced. Therefore, the 15 K difference is considered as an appropriate initial condition to initiate the temperature field within the solid liner domain. The sensitivity of the sulfuric acid formation and condensation to the initial temperature difference across the solid liner domain is studied in the next section. Based on the obtained results (not shown here), the temperature distribution on the interface at 90 CAD ATDC is almost uniform in the theta direction. Therefore, considering a boundary condition and initial condition which is only a function of z seems reasonable.

The effect of the initial temperature difference across the solid liner domain is negligible on the total produced mass of H_2SO_4 vapor (not shown) for the investigated case. This implies that the temperature distribution in the cylinder gas next to the liner is not highly affected by changing the solid liner initial temperature for the considered range of temperature distributions. On

the other hand, H_2SO_4 condensation shows a higher sensitivity to the solid-gas interface temperature. The variation of the liner area fraction above the piston where condensation of sulfuric acid may potentially occur (A_c/A) is presented in Figure 5 for the different initial temperature differences inside the solid liner domain. A_c is the liner area above the piston with potential condensation and A is the whole liner area above the piston. Potential liner surface area for sulfuric acid condensation is defined as the area on the liner surface with presence of H_2SO_4 vapor and a surface temperature lower than the sulfuric acid dew point. The sulfuric acid dew point is calculated using the correlation of Verhoff and Banchero [13]:

$$\begin{aligned}\frac{1}{T_{DP,a}} = 2.276 \times 10^{-3} - 2.943 \times 10^{-5} \ln(p_w) \\ -8.58 \times 10^{-5} \ln(p_a) + 6.20 \ln(p_w) \ln(p_a)\end{aligned} \tag{2}$$

where $T_{DP,a}$ is the dew point of sulfuric acid in Kelvin (K), while p_w and p_a are the partial pressures of water and sulfuric acid, respectively, in the unit millimetre of mercury (mmHg).

It can be seen from Figure 5 that there is no area with presence of H_2SO_4 and at the same time with a temperature below the dew point of sulfuric acid before 20 CAD ATDC for all cases. After 20 CAD ATDC, the liner surface area fraction with H_2SO_4 and temperature below the dew point starts to increase slightly and then decreases again. The reason for this reduction is a higher flame-wall interaction during the 30-35 CAD ATDC which leads to a higher wall temperature and a lower acid condensation. After 35 CAD ATDC, the potential sulfuric acid condensation increases continuously. This is because at higher CAD, the piston uncovers an increasingly colder liner

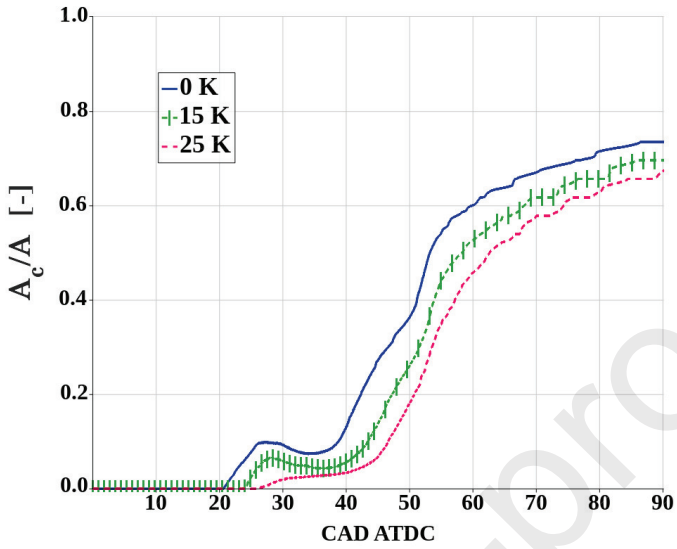

Figure 5: Fraction of liner surface area with potential sulfuric acid condensation (A_c/A) for different initial temperature differences across the liner domain.

surface. The 0 K case, which has the lowest interface temperature, shows the highest H_2SO_4 condensation and the lowest condensation is observed for the 25 K case.

To obtain insight into the formation and condensation of H_2SO_4, the spatial distribution of the mass fraction of sulfuric acid vapor (which is similar for the 0 K and 15 K cases at the solid-gas interface) and the liner surface area with potential sulfuric acid condensation is presented in Figure 6 for the 0 K and 15 K cases. Potential liner surface area for sulfuric acid condensation is depicted with red color. The sulfuric acid vapor is formed in the region where the local temperature is less than 600 K [1] while having sufficient amount of SO_3 and H_2O to form H_2SO_4 vapor. However, sulfuric acid condensation at a particular region can only occur when the local liner surface temperature

is lower than the H_2SO_4 dew point [1]. Therefore, as it can be seen in Figure 6, there are regions that contain a high concentration of H_2SO_4 vapor, but no condensation due to a high surface temperature. Without considering CHT calculations, the measured temperature 5 mm below the liner surface [12], should be applied on the liner surface as a boundary condition which is incorrect and would lead to a less accurate prediction of sulfuric acid condensation. On the other hand, in order to achieve an estimation of the solid-gas interface temperature based on the mentioned measured temperature, the initial temperature distribution should satisfy the balance between the mean value of the heat transfer to and from the solid liner domain. Therefore, these results (Figures 5 and 6) illustrate the importance of considering CHT calculations and initial temperature differences across the solid liner domain in order to achieve a better estimation of the liner surface temperature which is essential for prediction of the H_2SO_4 condensation.

3.3. Air humidity

In this section, the influence of air humidity on sulfuric acid formation and condensation is investigated. This is carried out by considering three cases with a water vapor mass fraction in the cylinder gas at the start of the simulation, i.e. at 0 CAD ATDC, of 0.5 % (base case), 2 % and 4 %, respectively, see Table 2. The total mass of the gas in the cylinder at the start of the simulation, i.e. the sum of the dry air mass and water mass, is assumed to be the same in all the cases. For all cases, the initial temperature difference of 15 K is considered across the solid liner domain. The list of reactions that participate in the sulfuric acid formation is presented in Table 3 (for more explanation about the reactions, please see our previous work [1]).

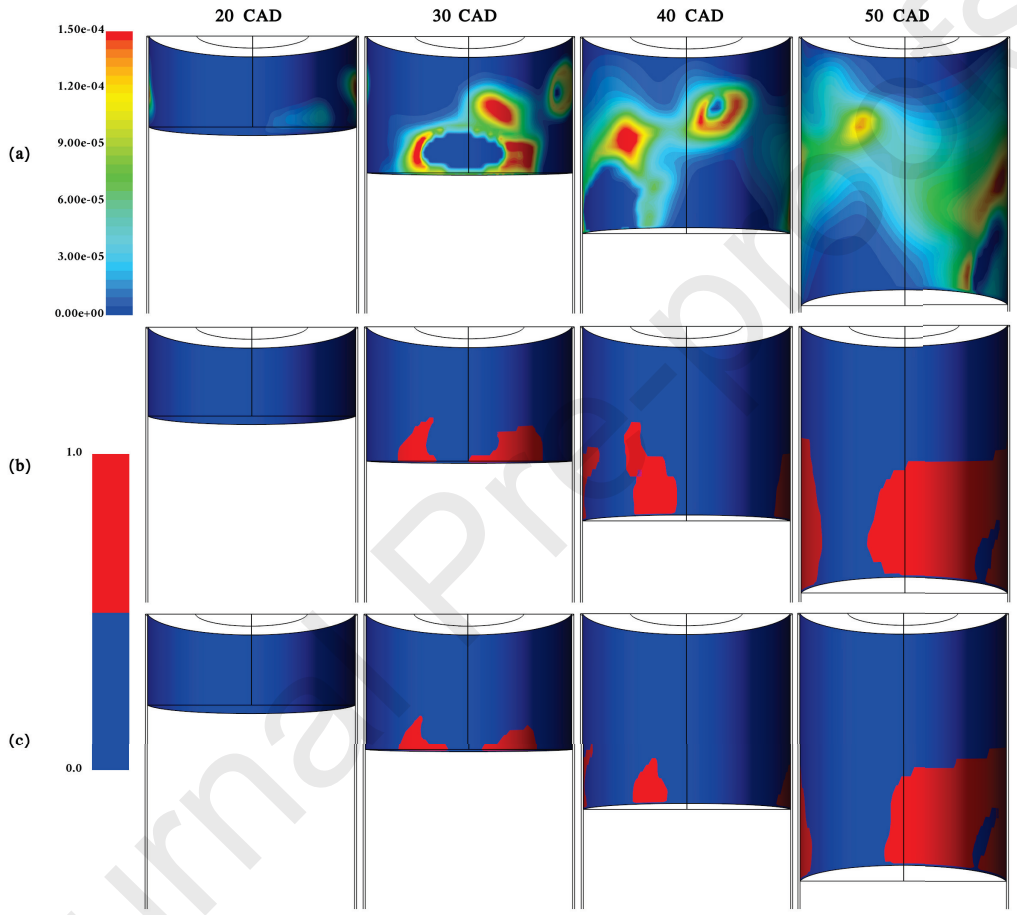

Figure 6: (a) Mass fraction of sulfuric acid vapor at the liner surface, (b) and (c) region of the liner surface with potential sulfuric acid condensation (red area): (b) initial temperature difference of 0 K; (c) initial temperature difference of 15 K.

Table 2: Mass fraction of species in the cylinder gas at the start of the simulation for different humidities.

H_2O mass fraction [%]	N_2 mass fraction [%]	O_2 mass fraction [%]
0.5	76.20	23.30
2.0	75.05	22.95
4.0	73.52	22.48

Table 3: Reactions of the skeletal sulphur model [2, 3].

No.	Reaction
1	$\mathrm{Fuel-S} + \mathrm{O_2} \rightarrow \mathrm{SO_2}$
2	$\mathrm{SO_2} + \mathrm{O(+M)} \leftrightarrow \mathrm{SO_3}$
3	$\mathrm{SO_3} + \mathrm{H} \leftrightarrow \mathrm{SO_2} + \mathrm{OH}$
4	$\mathrm{SO_2} + \mathrm{OH(+M)} \leftrightarrow \mathrm{HOSO_2(+M)}$
5	$\mathrm{HOSO_2} + \mathrm{O_2} \leftrightarrow \mathrm{HO_2} + \mathrm{SO_3}$
6	$\mathrm{SO_3} + \mathrm{H_2O} \leftrightarrow \mathrm{H_2SO_4}$

The variation in the averaged H_2SO_4 vapor mass fraction is presented in Figure 7 for the different initial water vapor concentrations. As it can be seen, the sulfuric acid formation changes considerably by varying the humidity. The averaged H_2SO_4 vapor inside the cylinder at 90 CAD ATDC increases 45 % and 148 % by increasing the humidity to 2 % and 4 %, respectively, in comparison with the 0.5 % humidity case.

H_2SO_4 is formed through the reaction between SO_3 and H_2O cf. Table 3. It is noteworthy that there is no significant difference in the averaged SO_3 mass fraction for the different levels of humidity (not shown). Therefore, the main reason for the increase in the sulfuric acid formation is the increased water vapor content inside the cylinder (please see reaction 6). The spatial distribution of H_2SO_4 vapor on the solid-gas interface is illustrated for the three different water vapor concentrations in Figure 8 at 20, 30 and 40 CAD ATDC. As it can be seen, the mass fraction of H_2SO_4 vapor for the 4 % case is higher than the other cases. Furthermore, the flame-wall interaction is different, especially for the 4 % H_2O case based on the regions with zero mass fraction of H_2SO_4 with in the mass fraction contours which indicate the regions with high temperature and flame-wall interaction.

Figure 9 illustrates the variation of the liner area fraction above the piston where condensation of sulfuric acid may potentially occur (A_c/A) for the different amounts of water vapor in the cylinder gas at the start of the simulation. Based on the results, the potential condensation of sulfuric acid on the liner increases with increasing water vapor mass fraction. The predicted H_2SO_4 vapor and condensed H_2SO_4 values at 90 CAD ATDC for the different water vapor amounts in the the cylinder gas at the start of the simulation

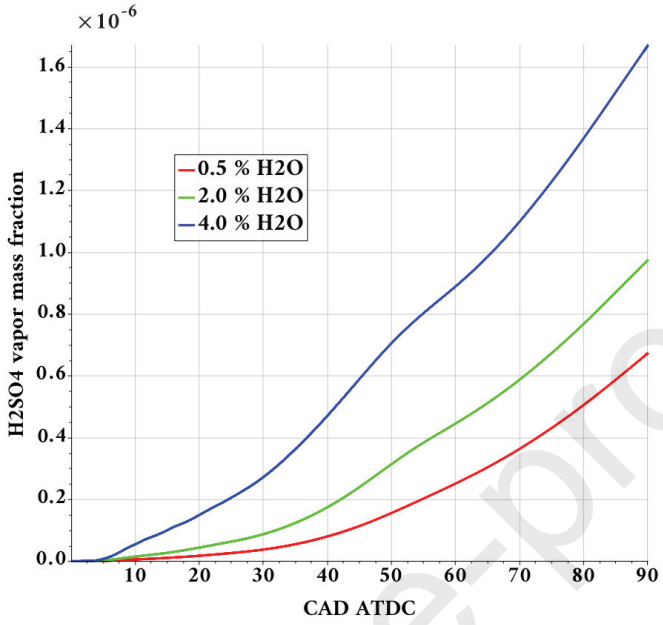

Figure 7: Spatially averaged sulfuric acid vapor mass fraction inside the cylinder.

are summarised in Table 4. By comparing the sulfuric acid formation and condensation results it can be concluded that the influence of water vapor on sulfuric acid formation is higher than its effect on sulfuric acid condensation. For instance, by increasing the water vapor mass fraction from 0.5 % to 4 %, the sulfuric acid vapor formation increases about 150 %, while the region of the liner surface with potential sulfuric acid condensation is increased about 6 %.

4. Conclusion

With the aim to achieve an estimation of sulfuric acid formation and condensation under large two-stroke marine engine like conditions, conjugate heat transfer calculations are coupled with a CFD simulation. Different ini-

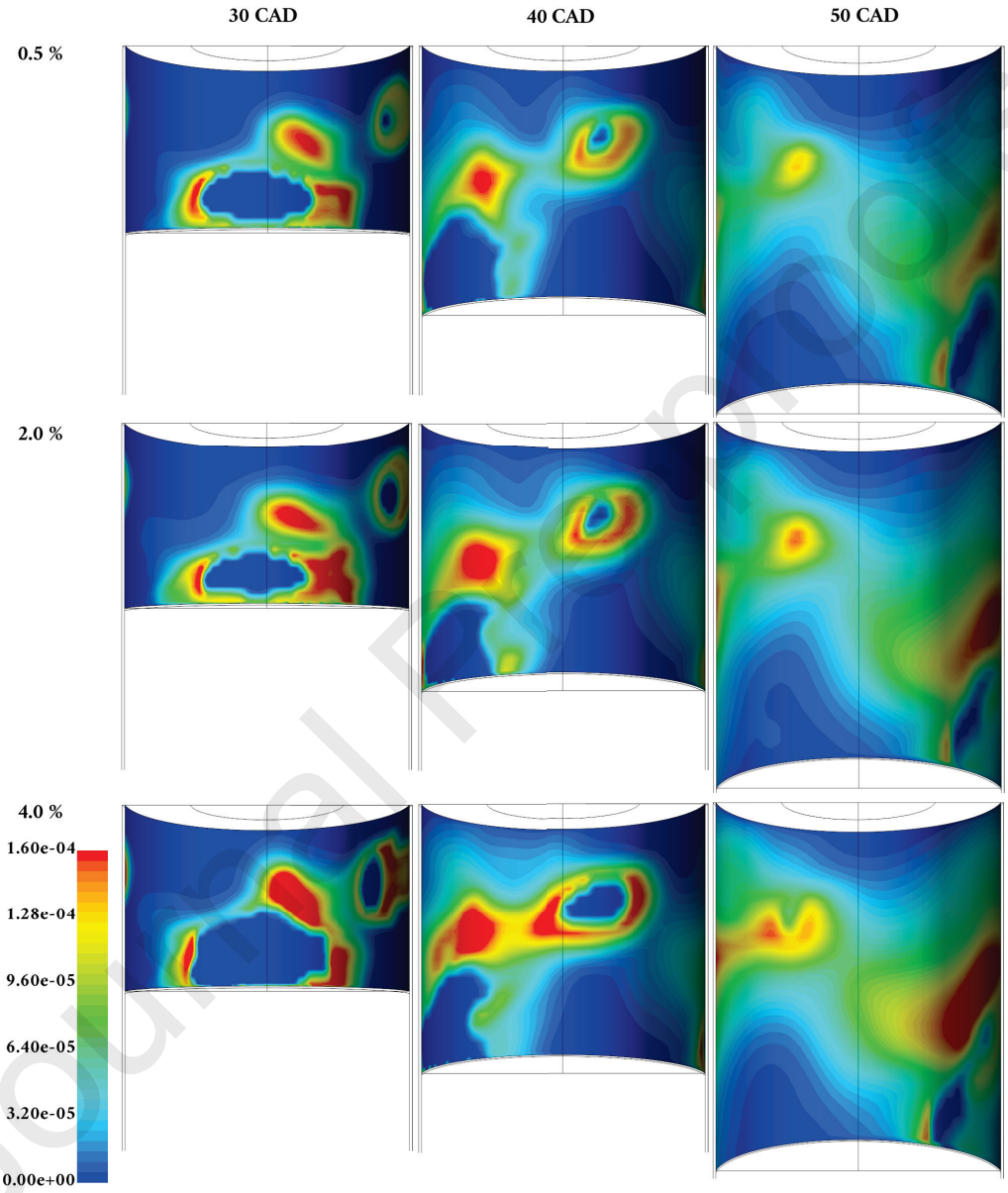

Figure 8: Mass fraction of sulfuric acid vapor on the solid-gas interface for 0.5%, 2% and 4% of water vapor in the cylinder gas at the start of the simulation.

Table 4: The simulated spatially averaged H_2SO_4 vapor and condensed H_2SO_4 values at 90 CAD ATDC.

H_2O mass fraction [%]	H_2SO_4 vapor [ppmw]	A_c/A [%]
0.5	0.7	69.5
2.0	1.0	72.0
4.0	1.7	73.4

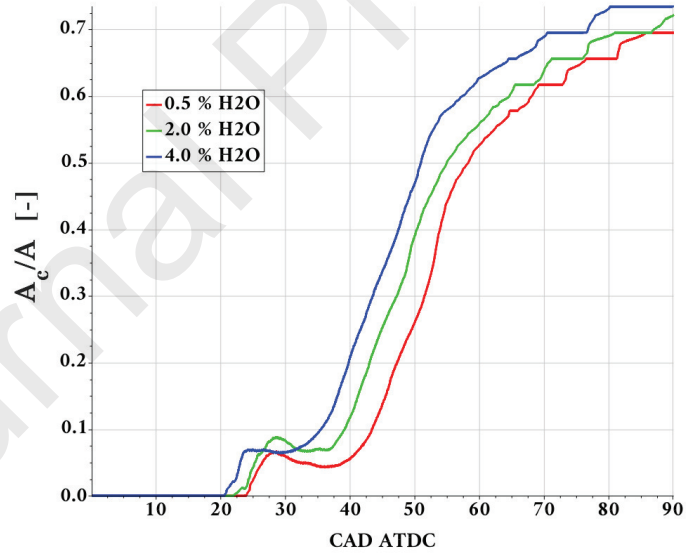

Figure 9: Fraction of liner surface area with potential sulfuric acid condensation (A_c/A) for different water vapor mass fractions in the cylinder gas at the start of the simulation.

tial temperature differences across the liner domain are considered to achieve an appropriate estimation of the temperature distribution inside the liner. This is carried out to mimic the accumulated effect of previous cycles on the internal temperature of the liner. It is found that a 15 K temperature difference across the 5 mm thickness of liner is an appropriate initial condition which satisfies the energy balance inside the liner. Based on the results, the temperature distribution inside the liner does not have a considerable effect on the H_2SO_4 formation but it changes the H_2SO_4 condensation. The results of the spatial distribution of H_2SO_4 vapor suggest that there is no condensation of H_2SO_4 in certain regions on the liner despite the presence of H_2SO_4 vapor due to a high temperature. The sensitivity of H_2SO_4 formation and condensation to the amount of water vapor in the air is studied to investigate the effect of ambient air conditions on H_2SO_4 formation and condensation under large two-stroke marine engine like conditions. It is concluded that an increasing humidity has a significant effect on the formation of H_2SO_4, while the effect on the condensation process is less pronounced. By increasing the water vapor mass fraction from 0.5 % to 4 %, the sulfuric acid vapor formation and condensation at 90 CAD ATDC increase about 150 % and 6 %, respectively.

5. Acknowledgment

The authors gratefully acknowledge the financial support from the Independent Research Fund Denmark (DFF) and MAN Energy Solutions under the grant number 8022-00143B and funding from A/S D/S Orient's Fond. The authors also would like to thank MAN Energy Solutions, Denmark for

sharing the experimental data. The computations were performed using the Niflheim cluster at the Technical University of Denmark (DTU).

References

[1] K. M. Pang, N. Karvounis, J. H. Walther, J. Schramm, P. Glarborg, S. Mayer, Modeling of temporal and spatial evolution of sulphur oxides and sulphuric acid under large, two-stroke marine engine-like conditions using integrated CFD-chemical kinetics, Appl. Energy 193 (2017) 63–73.

[2] L. Hindiyarti, P. Glarborg, P. Marshall, Reactions of SO_3 with the O/H radical pool under combustion conditions, J. Phys. Chem. A 111 (2007) 3984–3991.

[3] R. Cordtz, J. Schramm, A. Andreasen, S. S. Eskildsen, S. Mayer, Modeling the distribution of sulfur compounds in a large two stroke diesel engine, Energy & Fuels 27 (2013) 1652–1660.

[4] K. M. Pang, N. Karvounis, J. H. Walther, J. Schramm, Numerical investigation of soot formation and oxidation processes under large two-stroke marine diesel engine-like conditions using integrated CFD-chemical kinetics, Appl. Energy 169 (2016) 874–887.

[5] N. Karvounis, K. M. Pang, S. Mayer, J. H. Walther, Numerical simulation of condensation of sulfuric acid and water in a large two-stroke marine diesel engine, Appl. Energy 211 (2018) 1009–1020.

[6] M. V. Jensen, N. Karvounis, K. M. Pang, J. C. Ong, J. H. Walther, Numerical investigation of the effect of conjugate heat transfer on sul-

furic acid condensation in a large two-stroke marine diesel engine, in: HEFAT 2019, HEFAT, 14th International Conference on Heat Transfer, Fluid Mechanics and Thermodynamics, Wicklow, Ireland, 2019.

[7] Y. Li, S. Kong, Coupling conjugate heat transfer with in-cylinder combustion modeling for engine simulation, Int. J. Heat Mass Transfer 54 (11-12) (2011) 2467–2478.

[8] L. Zhang, Parallel simulation of engine in-cylinder processes with conjugate heat transfer modeling, Appl. Thermal Engng. 142 (2018) 232–240.

[9] L. Vinceković, Numerical simulation of a piston cooling of a two-stroke marine diesel engine with experimental validation, Master's thesis, Aalborg University (June 2018).

[10] F. Berni, G. Cicalese, S. Fontanesi, A modified thermal wall function for the estimation of gas-to-wall heat fluxes in cfd in-cylinder simulations of high performance spark-ignition engine, Appl. Thermal Engng. 115 (2017) 1045–1062.

[11] F. R. Menter, Two-equation eddy-viscosity turbulence modeling for engineering applications, AIAA J. 32 (8) (1994) 1598–1605.

[12] E. Sigurdsson, K. M. Ingvorsen, M. V. Jensen, S. Mayer, S. Matlok, J. H. Walther, Numerical analysis of scavenge flow and convective heat transfer in large two-stroke marine diesel engines, Appl. Energy 123 (2014) 37–46.

[13] F. H. Verhoff, J. T. Banchero, Predicting dew points of flue gases, Chem. Engng. Prog. 70 (1974) 71–72.